

Protein J (2008) 27:276–282  
DOI 10.1007/s10930-008-9135-2

# Benzene-di-*N*-Substituted Carbamates as Conformationally Constrained Substrate Analogs of Cholesterol Esterase

S.-Y. Chiou · M.-C. Lin · M.-T. Hwang ·  
H.-G. Chang · G. Lin

Published online: 14 May 2008  
© Springer Science+Business Media, LLC 2008

**Abstract** Benzene-1,2-, 1,3-, and 1,4-di-*N*-substituted carbamates (**1–15**) are synthesized as the constrained analogs of *gauche*, *eclipsed*, and *anti* conformations, respectively, for the glycerol backbones of triacylglycerol. Carbamates **1–15** are characterized as the pseudo substrate inhibitors of cholesterol esterase. Long chain carbamates are more potent inhibitors than short chain ones. Comparison of different geometries for benzene-di-substituted carbamates, such as benzene-1,2-di-*N*-octylcarbamate (**3**) (*ortho*-**3**), benzene-1,3-di-*N*-octylcarbamate (**8**) (*meta*-**8**), and benzene-1,4-di-*N*-octylcarbamates (**13**) (*para*-**13**), indicates that inhibitory potencies are as followed: *meta*-**8** > *para*-**13** > *ortho*-**3**. Therefore, we suggest that the preferable conformation for the C(*sn*-1)–O/C(*sn*-2)–O glycerol backbone in the enzyme–triacylglycerol complex is the *eclipsed* conformation. Meanwhile, kinetic data indicate that among *ortho*, *meta*, and *para* carbamates, *meta* carbamates most resemble the substrate cholesterol ester.

**Keywords** Cholesterol esterase · Inhibitor · Carbamate · Conformation

## Abbreviations

ACS	Acyl chain binding site
CEase	Cholesterol esterase
LDL	Low-density lipoprotein
PNPB	<i>p</i> -nitrophenyl butyrate
TX	Triton-X 100

## 1 Introduction

Cholesterol esterase (CEase, EC 3.1.1.13) also known as bile salt-activated lipase, carboxyl ester lipase, lysophospholipase, and non-specific lipase, is responsible for the hydrolysis of dietary cholesterol esters, fat soluble vitamin esters, phospholipids and triacylglycerols. Like the serine proteases, CEase possesses a catalytic triad, Ser194–His435–Asp320, that serves as a nucleophilic and general acid–base catalytic entity [1–3]. Two X-ray structures of CEase have been reported [4, 5]. Although different bile salt-activation mechanisms are proposed, the active site of CEase from two different X-ray crystal structures is similar to that of lipases.

CEase has also been demonstrated that it is involved directly in lipoprotein metabolism, in that the enzyme catalyzes the conversion of large low-density lipoprotein (LDL) to smaller, denser, more cholesterol ester-rich lipoproteins, and that the enzyme may regulate serum cholesterol levels [6]. Therefore, the ability of CEase to convert large LDL to smaller LDL subspecies, and the relationship between plasma CEase and LDL levels, suggest that high plasma CEase levels may constitute a potential risk factor for atherosclerosis. Thus, CEase inhibitors may be suitable for the treatment of combined lipoprotein disorders characterized by elevation of cholesterol [7–10].

S.-Y. Chiou  
Division of Neurosurgery, Chung Shan Medical University  
Hospital, Taichung 402, Taiwan

M.-C. Lin  
Department of Cardiology, Chung Shan Medical University  
Hospital, Taichung 402, Taiwan

M.-T. Hwang · H.-G. Chang · G. Lin (✉)  
Department of Chemistry, National Chung-Hsing University,  
Taichung 402, Taiwan  
e-mail: gilind@dragon.nchu.edu.tw

Aryl carbamates have been characterized as the pseudo substrate inhibitors of CEase [11–14]. We have reported that benzene-1,2-di-*N*-substituted carbamates (**1–5**) (*ortho* carbamates), benzene-1,3-di-*N*-substituted carbamates (**6–10**) (*meta* carbamates), and benzene-1,4-di-*N*-substituted carbamates (**11–15**) (*para* carbamates) are the conformationally constrained analogs of *gauche*, *eclipsed*, and *anti* conformations (Fig. 1), respectively, for the glycerol backbones of glycerol lipid such as phosphatidylcholine in the phospholipase A2 catalysis [15, 16]. Since CEase also catalyzes the hydrolysis of triacylglycerol, conformations for the glycerol backbone of substrate may also play an important role in the CEase catalysis. Therefore, we report here that benzene-di-*N*-substituted carbamates

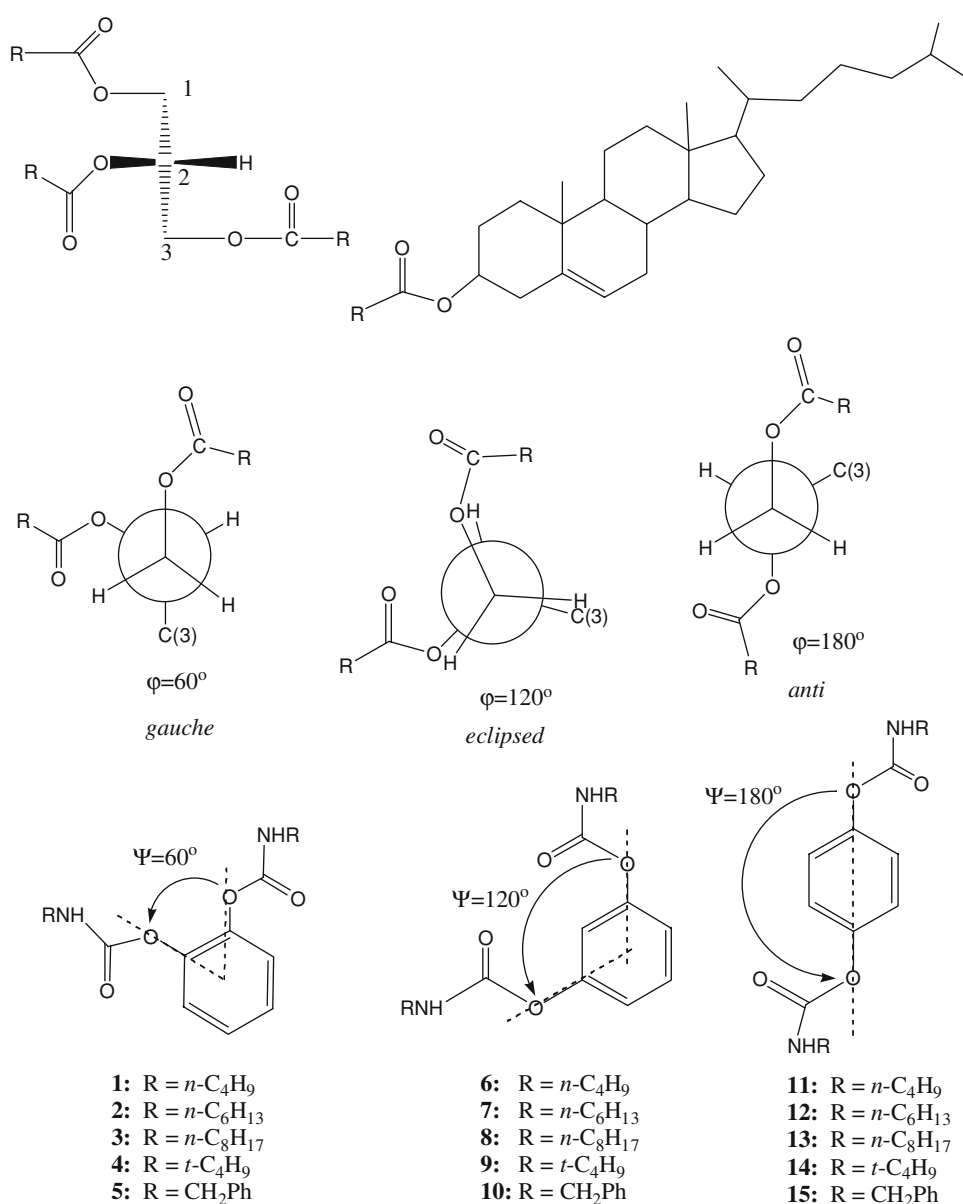
(**1–15**) (Fig. 1) act as the conformationally constrained analogs of *gauche*, *eclipsed*, and *anti* conformations, respectively, for the glycerol backbones of triacylglycerol (substrate).

## 2 Materials and Methods

### 2.1 Materials

Porcine pancreatic CEase, *p*-nitrophenyl butyrate (PNPB), and triton-X 100 (TX) were obtained from Sigma. All other chemicals were of the highest purity available commercially.

**Fig. 1** Three conformations for the glycerol backbones of triacylglycerol and chemical structures of cholesterol ester and carbamates **1–15**



## 2.2 Synthesis of Inhibitors

Benzene-1,2-, 1,3-, and 1,4-di-*N*-substituted carbamates (**1–15**) (Fig. 1) were synthesized from the condensation of catechol, resorcinol, and hydroquinone, respectively, with three equivalents of the corresponding isocyanate in triethylamine at 25 °C for 24 h (65–90% yield) [17, 18]. The products were purified by liquid chromatography (silica gel, hexane-ethyl acetate) and characterized by  $^1\text{H}$  and  $^{13}\text{C}$  NMR spectra.

### 2.2.1 Benzene-1,2-di-*N*-*n*-butylcarbamate (**1**)

$^1\text{H}$  NMR ( $\text{CDCl}_3$ , 400 MHz)  $\delta/\text{ppm}$  0.93 (t,  $J = 7$  Hz, 6H,  $\omega\text{-CH}_3$ ), 1.35 (sextet,  $J = 7$  Hz, 4H,  $\gamma\text{-CH}_2$ ), 1.52 (quintet,  $J = 7$  Hz, 4H,  $\beta\text{-CH}_2$ ), 3.24 (q,  $J = 7$  Hz, 4H,  $\alpha\text{-CH}_2$ ), 5.09 (s, 2H, NH), and 7.15–7.24 (m, 4H, benzene *H*'s).  $^{13}\text{C}$  NMR ( $\text{CDCl}_3$ , 100 MHz, assignment from DEPT experiments)  $\delta/\text{ppm}$  13.5 ( $\omega\text{-CH}_3$ ), 19.6 ( $\gamma\text{-CH}_2$ ), 31.6 ( $\beta\text{-CH}_2$ ), 40.8 ( $\alpha\text{-CH}_2$ ), 123.4 (*C*-4 and *C*-5 of the benzene ring), 125.8 (*C*-3 and *C*-6 of the benzene ring), 143.0 (*C*-1 and *C*-2 of the benzene ring), and 153.9 (carbamate  $\text{C}=\text{O}$ ).

### 2.2.2 Benzene-1,2-di-*N*-*n*-hexylcarbamate (**2**)

$^1\text{H}$  NMR ( $\text{CDCl}_3$ , 400 MHz)  $\delta/\text{ppm}$  0.88 (t,  $J = 7$  Hz, 6H,  $\omega\text{-CH}_3$ ), 1.26–1.35 (m, 12H,  $\gamma$ - to  $\omega\text{-1-CH}_2$ ), 1.51–1.55 (m, 4H,  $\beta\text{-CH}_2$ ), 3.23 (q,  $J = 7$  Hz, 4H,  $\alpha\text{-CH}_2$ ), 5.08 (s, 2H, NH), and 7.15–7.24 (m, 4H, benzene *H*'s).  $^{13}\text{C}$  NMR ( $\text{CDCl}_3$ , 100 MHz, assignment from DEPT experiments)  $\delta/\text{ppm}$  13.9 ( $\omega\text{-CH}_3$ ), 22.4, 26.3, 29.6 ( $\gamma$ -,  $\delta$ -, and  $\varepsilon\text{-CH}_2$ ), 31.3 ( $\beta\text{-CH}_2$ ), 41.2 ( $\alpha\text{-CH}_2$ ), 123.4 (*C*-4 and *C*-5 of the benzene ring), 125.9 (*C*-3 and *C*-6 of the benzene ring), 143.0 (*C*-1 and *C*-2 of the benzene ring), and 153.9 (carbamate  $\text{C}=\text{O}$ ).

### 2.2.3 Benzene-1,2-di-*N*-*n*-octylcarbamate (**3**)

$^1\text{H}$  NMR ( $\text{CDCl}_3$ , 400 MHz)  $\delta/\text{ppm}$  0.89 (t,  $J = 7$  Hz, 6H,  $\omega\text{-CH}_3$ ), 1.26–1.30 (m, 20H,  $\gamma$ - to  $\omega\text{-1-CH}_2$ ), 1.51–1.57 (m, 4H,  $\beta\text{-CH}_2$ ), 3.23 (q,  $J = 7$  Hz, 4H,  $\alpha\text{-CH}_2$ ), 5.06 (s, 2H, NH), and 7.15–7.24 (m, 4H, benzene *H*'s).  $^{13}\text{C}$  NMR ( $\text{CDCl}_3$ , 100 MHz, assignment from DEPT experiments)  $\delta/\text{ppm}$  14.0 ( $\omega\text{-CH}_3$ ), 22.5, 26.2, 26.3, 29.1, 29.7 ( $\gamma$ - to  $\omega\text{-1-CH}_2$ ), 31.7 ( $\beta\text{-CH}_2$ ), 41.2 ( $\alpha\text{-CH}_2$ ), 123.4 (*C*-4 and *C*-5 of the benzene ring), 126.0 (*C*-3 and *C*-6 of the benzene ring), 143.0 (*C*-1 and *C*-2 of the benzene ring), and 153.9 (carbamate  $\text{C}=\text{O}$ ).

### 2.2.4 Benzene-1,2-di-*N*-*t*-butylcarbamate (**4**)

$^1\text{H}$  NMR ( $\text{CDCl}_3$ , 400 MHz)  $\delta/\text{ppm}$  1.36 (s, 18H,  $\text{CH}_3$ ), 5.09 (s, 2H, NH), and 7.15–7.24 (m, 4H, benzene *H*'s).  $^{13}\text{C}$

NMR ( $\text{CDCl}_3$ , 100 MHz, assignment from DEPT experiments)  $\delta/\text{ppm}$  28.7 ( $\text{CH}_3$ ), 50.8 ( $\text{C}(\text{CH}_3)_3$ ), 123.5 (*C*-4 and *C*-5 of the benzene ring), 125.9 (*C*-3 and *C*-6 of the benzene ring), 142.9 (*C*-1 and *C*-2 of the benzene ring), and 151.8 (carbamate  $\text{C}=\text{O}$ ).

### 2.2.5 Benzene-1,2-di-*N*-benzylcarbamate (**5**)

$^1\text{H}$  NMR ( $\text{CDCl}_3$ , 400 MHz)  $\delta/\text{ppm}$  4.33 (d,  $J = 6$  Hz, 4H,  $\text{CH}_2\text{Ph}$ ), 5.09 (s, 2H, NH), and 7.15–7.24 (m, 4H, 1,2-benzene *H*'s), 7.27–7.30 (m, 10H, phenyl *H*'s of the benzyl group).  $^{13}\text{C}$  NMR ( $\text{CDCl}_3$ , 100 MHz, assignment from DEPT experiments)  $\delta/\text{ppm}$  45.3 (benzyl  $\text{CH}_2$ ), 123.5, 126.2, 127.4, 127.7, 128.6, 138.1, 142.9 (aromatic *C*'s), and 153.9 (carbamate  $\text{C}=\text{O}$ ).

### 2.2.6 Benzene-1,3-di-*N*-*n*-butylcarbamate (**6**)

$^1\text{H}$  NMR ( $\text{CDCl}_3$ , 400 MHz)  $\delta/\text{ppm}$  0.93 (t,  $J = 7$  Hz, 6H,  $\omega\text{-CH}_3$ ), 1.37 (sextet,  $J = 7$  Hz, 4H,  $\gamma\text{-CH}_2$ ), 1.52 (quintet,  $J = 7$  Hz, 4H,  $\beta\text{-CH}_2$ ), 3.24 (q,  $J = 7$  Hz, 4H,  $\alpha\text{-CH}_2$ ), 4.99 (s, 2H, NH), and 6.90–7.40 (m, 4H, benzene *H*'s).  $^{13}\text{C}$  NMR ( $\text{CDCl}_3$ , 100 MHz, assignment from DEPT experiments)  $\delta/\text{ppm}$  13.5 ( $\omega\text{-CH}_3$ ), 19.7 ( $\gamma\text{-CH}_2$ ), 31.6 ( $\beta\text{-CH}_2$ ), 40.7 ( $\alpha\text{-CH}_2$ ), 115.3 (*C*-5 of the benzene ring), 118.0 (*C*-4 and *C*-6 of benzene ring), 129.0 (*C*-2 of the benzene ring), 151.4 (*C*-1 and *C*-3 of the benzene ring), and 154.2 (carbamate  $\text{C}=\text{O}$ ).

### 2.2.7 Benzene-1,3-di-*N*-*n*-hexylcarbamate (**7**)

$^1\text{H}$  NMR ( $\text{CDCl}_3$ , 400 MHz)  $\delta/\text{ppm}$  0.88 (t,  $J = 7$  Hz, 6H,  $\omega\text{-CH}_3$ ), 1.30–1.35 (m, 12H,  $\gamma$ - to  $\omega\text{-1-CH}_2$ ), 1.52–1.57 (m, 4H,  $\beta\text{-CH}_2$ ), 3.23 (q,  $J = 7$  Hz, 4H,  $\alpha\text{-CH}_2$ ), 4.98 (s, 2H, NH), and 6.90–7.35 (m, 4H, benzene *H*'s).  $^{13}\text{C}$  NMR ( $\text{CDCl}_3$ , 100 MHz, assignment from DEPT experiments)  $\delta/\text{ppm}$  13.9 ( $\omega\text{-CH}_3$ ), 22.4, 26.3, 29.6 ( $\gamma$ -,  $\delta$ -, and  $\varepsilon\text{-CH}_2$ ), 31.3 ( $\beta\text{-CH}_2$ ), 41.2 ( $\alpha\text{-CH}_2$ ), 115.3 (*C*-5 of the benzene ring), 118.1 (*C*-4 and *C*-6 of the benzene ring), 129.1 (*C*-2 of the benzene ring), 151.4 (*C*-1 and *C*-3 of the benzene ring), and 154.2 (carbamate  $\text{C}=\text{O}$ ).

### 2.2.8 Benzene-1,3-di-*N*-*n*-octylcarbamate (**8**)

$^1\text{H}$  NMR ( $\text{CDCl}_3$ , 400 MHz)  $\delta/\text{ppm}$  0.88 (t,  $J = 7$  Hz, 6H,  $\omega\text{-CH}_3$ ), 1.26–1.33 (m, 20H,  $\gamma$ - to  $\omega\text{-1-CH}_2$ ), 1.52–1.57 (m, 4H,  $\beta\text{-CH}_2$ ), 3.23 (q,  $J = 7$  Hz, 4H,  $\alpha\text{-CH}_2$ ), 4.97 (s, 2H, NH), and 6.90–7.35 (m, 4H, benzene *H*'s).  $^{13}\text{C}$  NMR ( $\text{CDCl}_3$ , 100 MHz, assignment from DEPT experiments)  $\delta/\text{ppm}$  14.0 ( $\omega\text{-CH}_3$ ), 22.6, 26.7, 29.1, 29.2, 29.7 ( $\gamma$ - to  $\omega\text{-1-CH}_2$ ), 31.7 ( $\beta\text{-CH}_2$ ), 41.2 ( $\alpha\text{-CH}_2$ ), 115.3 (*C*-5 of the benzene ring), 118.2 (*C*-4 and *C*-6 of the benzene ring), 129.2 (*C*-2 of the benzene ring), 151.5 (*C*-1 and *C*-3 of the benzene ring), and 154.2 (carbamate  $\text{C}=\text{O}$ ).

### 2.2.9 Benzene-1,3-di-*N*-*t*-butylcarbamate (**9**)

$^1\text{H}$  NMR ( $\text{CDCl}_3$ , 400 MHz)  $\delta/\text{ppm}$  1.36 (s, 18 H,  $\text{CH}_3$ ), 5.09 (s, 2H, NH), and 6.90–7.35 (m, 4H, benzene  $H$ 's).  $^{13}\text{C}$  NMR ( $\text{CDCl}_3$ , 100 MHz, assignment from DEPT experiments)  $\delta/\text{ppm}$  28.7 ( $\text{CH}_3$ ), 50.8 ( $\text{C}(\text{CH}_3)_3$ ), 115.3 ( $C$ -5 of the benzene ring), 118.3 ( $C$ -4 and  $C$ -6 of the benzene ring), 129.2 ( $C$ -2 of benzene ring), 151.3 ( $C$ -1 and  $C$ -3 of the benzene ring), and 152.3 (carbamate  $\text{C}=\text{O}$ ).

### 2.2.10 Benzene-1,3-di-*N*-benzylcarbamate (**10**)

$^1\text{H}$  NMR ( $\text{CDCl}_3$ , 400 MHz)  $\delta/\text{ppm}$  4.43 (d,  $J = 2$  Hz, 4H,  $\text{CH}_2\text{Ph}$ ), 5.09 (s, 2H, NH), 6.90–7.35 (m, 4H, benzene  $H$ 's), and 7.27–7.37 (m, 10H, phenyl  $H$ 's of the benzyl group).  $^{13}\text{C}$  NMR ( $\text{CDCl}_3$ , 100 MHz, assignment from DEPT experiments)  $\delta/\text{ppm}$  45.3 (benzyl  $\text{CH}_2$ ), 115.3, 118.4, 127.7, 127.8, 128.8, 129.4, 137.9, 151.4 (aromatic  $C$ 's), and 154.2 (carbamate  $\text{C}=\text{O}$ ).

### 2.2.11 Benzene-1,4-di-*N*-*n*-butylcarbamate (**11**)

$^1\text{H}$  NMR ( $\text{CDCl}_3$ , 400 MHz)  $\delta/\text{ppm}$  0.93 (t,  $J = 7$  Hz, 6H,  $\omega$ - $\text{CH}_3$ ), 1.37 (sextet,  $J = 7$  Hz, 4H,  $\gamma$ - $\text{CH}_2$ ), 1.53 (quintet,  $J = 7$  Hz, 4H,  $\beta$ - $\text{CH}_2$ ), 3.24 (q,  $J = 7$  Hz, 4H,  $\alpha$ - $\text{CH}_2$ ), 4.98 (s, 2H, NH), and 7.07 (s, 4H, benzene  $H$ 's).  $^{13}\text{C}$  NMR ( $\text{CDCl}_3$ , 100 MHz, assignment from DEPT experiments)  $\delta/\text{ppm}$  13.7 ( $\omega$ - $\text{CH}_3$ ), 19.9 ( $\gamma$ - $\text{CH}_2$ ), 31.8 ( $\beta$ - $\text{CH}_2$ ), 40.9 ( $\alpha$ - $\text{CH}_2$ ), 122.2 ( $C$ -2,  $C$ -3,  $C$ -5 and  $C$ -6 of the benzene ring), 148.0 ( $C$ -1 and  $C$ -4 of the benzene ring), and 154.5 (carbamate  $\text{C}=\text{O}$ ).

### 2.2.12 Benzene-1,4-di-*N*-*n*-hexylcarbamate (**12**)

$^1\text{H}$  NMR ( $\text{CDCl}_3$ , 400 MHz)  $\delta/\text{ppm}$  0.88 (t,  $J = 7$  Hz, 6H,  $\omega$ - $\text{CH}_3$ ), 1.30–1.35 (m, 12H,  $\gamma$ - to  $\omega$ -1- $\text{CH}_2$ ), 1.52–1.55 (m, 4H,  $\beta$ - $\text{CH}_2$ ), 3.24 (q,  $J = 7$  Hz, 4H,  $\alpha$ - $\text{CH}_2$ ), 4.97 (s, 2H, NH), and 7.07 (s, 4H, benzene  $H$ 's).  $^{13}\text{C}$  NMR ( $\text{CDCl}_3$ , 100 MHz, assignment from DEPT experiments)  $\delta/\text{ppm}$  14.0 ( $\omega$ - $\text{CH}_3$ ), 22.5, 26.4, 29.7 ( $\gamma$ -,  $\delta$ -, and  $\varepsilon$ - $\text{CH}_2$ ), 31.4 ( $\beta$ - $\text{CH}_2$ ), 41.3 ( $\alpha$ - $\text{CH}_2$ ), 122.2 ( $C$ -2,  $C$ -3,  $C$ -5 and  $C$ -6 of the benzene ring), 148.0 ( $C$ -1 and  $C$ -4 of the benzene ring), and 154.5 (carbamate  $\text{C}=\text{O}$ ).

### 2.2.13 Benzene-1,4-di-*N*-*n*-octylcarbamate (**13**)

$^1\text{H}$  NMR ( $\text{CDCl}_3$ , 400 MHz)  $\delta/\text{ppm}$  0.87 (t,  $J = 7$  Hz, 6H,  $\omega$ - $\text{CH}_3$ ), 1.26–1.30 (m, 20H,  $\gamma$ - to  $\omega$ -1- $\text{CH}_2$ ), 1.52–1.55 (m, 4H,  $\beta$ - $\text{CH}_2$ ), 3.24 (q,  $J = 7$  Hz, 4H,  $\alpha$ - $\text{CH}_2$ ), 4.97 (s, 2H, NH), and 7.07 (s, 4H, benzene  $H$ 's).  $^{13}\text{C}$  NMR ( $\text{CDCl}_3$ , 100 MHz, assignment from DEPT experiments)  $\delta/\text{ppm}$  14.0 ( $\omega$ - $\text{CH}_3$ ), 22.6, 26.7, 29.1, 29.2, 29.8 ( $\gamma$ - to  $\omega$ -1- $\text{CH}_2$ ), 31.7 ( $\beta$ - $\text{CH}_2$ ), 41.3 ( $\alpha$ - $\text{CH}_2$ ), 122.2 ( $C$ -2,  $C$ -3,  $C$ -5 and  $C$ -6

of the benzene ring), 148.0 ( $C$ -1 and  $C$ -4 of the benzene ring), and 154.5 (carbamate  $\text{C}=\text{O}$ ).

### 2.2.14 Benzene-1,4-di-*N*-*t*-butylcarbamate (**14**)

$^1\text{H}$  NMR ( $\text{CDCl}_3$ , 400 MHz)  $\delta/\text{ppm}$  1.36 (s, 18 H,  $\text{CH}_3$ ), 5.09 (s, 2 H, NH), and 7.06 (s, 4 H, benzene  $H$ 's).  $^{13}\text{C}$  NMR ( $\text{CDCl}_3$ , 100 MHz, assignment from DEPT experiments)  $\delta/\text{ppm}$  29.0 ( $\text{CH}_3$ ), 51.1 ( $\text{C}(\text{CH}_3)_3$ ), 122.6 ( $C$ -2,  $C$ -3,  $C$ -5 and  $C$ -6 of the benzene ring), 148.1 ( $C$ -1 and  $C$ -4 of the benzene ring), and 152.9 (carbamate  $\text{C}=\text{O}$ ).

### 2.2.15 Benzene-1,4-di-*N*-benzylcarbamate (**15**)

$^1\text{H}$  NMR ( $\text{CDCl}_3$ , 400 MHz)  $\delta/\text{ppm}$  4.34 (d,  $J = 6$  Hz, 4H,  $\text{CH}_2\text{Ph}$ ), 5.09 (s, 2H, NH), and 7.09 (s, 4H, 1,2-benzene  $H$ 's), 7.28–7.35 (m, 10H, phenyl  $H$ 's of the benzyl group).  $^{13}\text{C}$  NMR ( $\text{CDCl}_3$ , 100 MHz, assignment from DEPT experiments)  $\delta/\text{ppm}$  45.3 (benzyl  $\text{CH}_2$ ), 122.1 ( $C$ -2,  $C$ -3,  $C$ -5 and  $C$ -6 of the benzene ring), 127.4, 127.9, 128.7, 140.0 (phenyl  $C$ 's of the benzyl group), 149.0 ( $C$ -1 and  $C$ -4 of the benzene ring), and 154.9 (carbamate  $\text{C}=\text{O}$ ).

## 2.3 Instrumental Methods

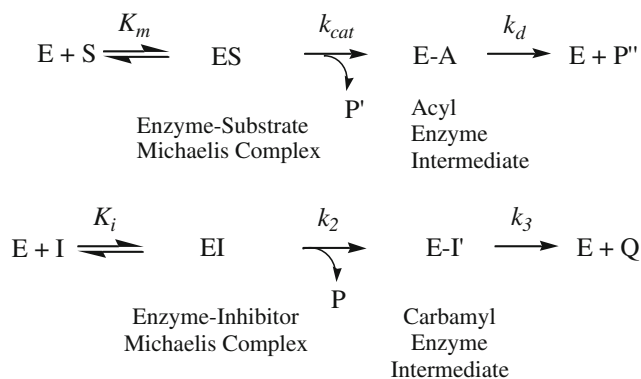
All steady state kinetic data were obtained from an UV–Visible spectrometer (Agilent 8453) with a cell holder circulated with a water bath.  $^1\text{H}$  and  $^{13}\text{C}$  NMR spectra were recorded in  $\text{CDCl}_3$  at 400 and 100 MHz, respectively, (Varian Gemini-400 spectrometer) with an internal reference tetramethylsilane at 25 °C.

## 2.4 Data Reduction

Origin (version 6.0) was used for linear and nonlinear least-squares curve fittings.

## 2.5 CEase Inhibition

CEase inhibition reactions were determined as described by Hosie et al [11–14]. CEase-catalyzed hydrolysis of PNPB in the presence of carbamates **1–15** was followed continuously at 410 nm on the UV–Visible spectrometer. The temperature was maintained at 25.0 °C by a refrigerated circulating water bath. All reactions were performed in sodium phosphate buffer (1 mL, 0.1 M, pH 7.0) containing NaCl (0.1 M),  $\text{CH}_3\text{CN}$  (2% by volume), detergent triton-X 100 (TX) (0.5% by weight), substrate PNPB (0.1 mM), and varying concentration of the inhibitors. Requisite volumes of stock solution of substrate PNPB and the inhibitor in acetonitrile were injected into reaction buffer via a pipet. CEase was dissolved in sodium



**Scheme 1** Kinetic scheme for pseudo substrate inhibitions of CEase by carbamates **1–15** in the presence of substrate. E: enzyme, CEase; E-A: acyl enzyme; EI: enzyme-inhibitor Michaelis complex; E-I': carbamyl enzyme; ES: enzyme-substrate Michaelis complex; I: pseudo substrate inhibitor, **1–15**;  $k_2$ : carbamyl constant;  $k_3$ : decarbamylation constant;  $k_{cat}$ : turnover number;  $k_d$ : deacylation constant;  $K_i$ : inhibition constant;  $K_m$ : Michaelis-Menten constant; P: product, 2-N-substituted-carbamylphenol; P': product, p-nitrophenol; P'': product, butyrate; Q: product, acylate; S: substrate, PNPB

phosphate buffer (0.1 M, pH 7.0). Carbamates **1–15** were characterized as the pseudo or alternate substrate inhibitors of CEase (Scheme 1) [11–14, 19, 20]. The carbamylation stage was rapid compared to subsequent decarbamylation ( $k_2 \gg k_3$ ), thus the two steps are easily resolved kinetically [11–13, 21]. The apparent inhibition constant ( $1 + [S]/K_m$ )  $K_i$  and carbamylation constant ( $k_2$ ) were obtained from the nonlinear least-squares curve fitting of the  $k_{app}$  vs.  $[I]$  plot against Eq. 1 (Fig. 2). The inhibition constant  $K_i$  was then calculated from the apparent inhibition constant when both  $[S]$  and  $K_m$  values for the CEase-catalyzed hydrolysis of PNPB were known (Table 1). The  $K_m$  value for the CEase catalyzed hydrolysis of PNPB was  $100 \pm 20 \mu\text{M}$  obtained from Michaelis–Menten equation. The bimolecular rate constant,  $k_i = k_2/K_i$ , was related to overall inhibitory potency.

$$k_{app} = k_2[I]/(K_i(1 + [S]/K_m) + [I]) \quad (1)$$

Duplicate sets of data were collected for each inhibitor concentration.

### 3 Results and Discussion

#### 3.1 Pseudo Substrate Inhibition of CEase by Carbamates **1–15**

Since the inhibition of CEase by carbamates **1–15** follows first-order kinetics over the observed time period for the steady-state kinetics, first-order rate constant,  $k_{app}$ , for pseudo substrate inhibition is determined from Eq. 1 [11–14, 19]. Therefore, carbamates **1–15** are characterized

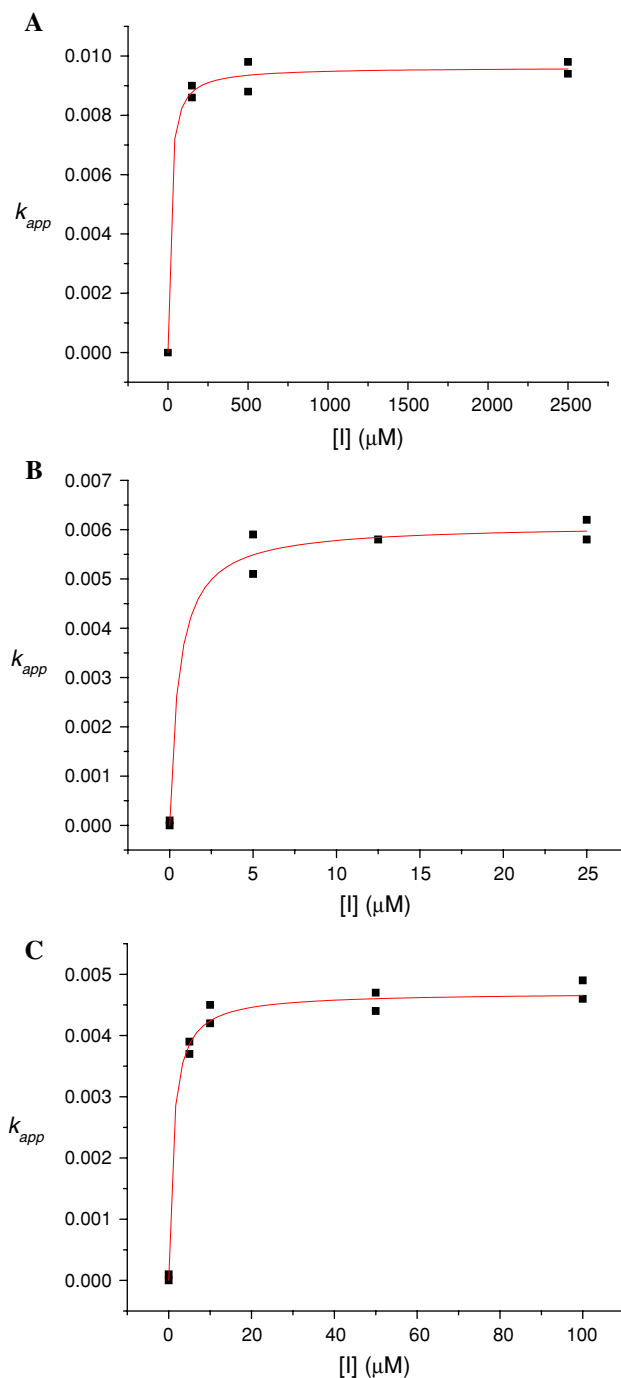


**Fig. 2** Nonlinear least-squares curve fittings of  $k_{app}$  vs. inhibitor concentration  $[I]$  plot against Eq. 1 for the pseudo-substrate inhibition [11–14] of CEase by (a) *ortho*-**3**, (b) *meta*-**8**, and (c) *para*-**13**. The parameters of the fit were (a)  $k_2 = 0.00096 \pm 0.00002 \text{ s}^{-1}$ ,  $K_i = 7 \pm 2 \mu\text{M}$ , and  $R^2 = 0.99483$ ; (b)  $k_2 = 0.00064 \pm 0.00003 \text{ s}^{-1}$ ,  $K_i = 0.4 \pm 0.1 \mu\text{M}$ , and  $R^2 = 0.99163$ ; and (c)  $k_2 = 0.00050 \pm 0.00001 \text{ s}^{-1}$ ,  $K_i = 0.7 \pm 0.1 \mu\text{M}$ , and  $R^2 = 0.99418$ . CEase-catalyzed hydrolysis of PNPB in the presence of carbamate **3**, **8** or **13** was followed continuously at 410 nm on the UV–Visible spectrometer at 25.0 °C. All reactions were performed in sodium phosphate buffer (1 mL, 0.1 M, pH 7.0) containing NaCl (0.1 M),  $\text{CH}_3\text{CN}$  (2% by volume), detergent triton-X 100 (TX) (0.5% by weight), substrate PNPB (0.1 mM), and varying concentration of the inhibitors

**Table 1** The  $k_2$ ,  $K_i$  and  $k_i$  values<sup>a</sup> of the CEase inhibitions by benzene-di-*N*-substituted carbamates (**1–15**)

Inhibitors	$K_i$ ( $\mu\text{M}$ )	$k_2$ ( $10^{-3} \text{ s}^{-1}$ )	$k_i$ ( $10^3 \text{ M}^{-1} \text{ s}^{-1}$ )
1	$27 \pm 4$	$7.0 \pm 0.2$	$0.27 \pm 0.03$
2	$20 \pm 2$	$12.4 \pm 0.2$	$0.61 \pm 0.08$
3	$7 \pm 2$	$9.6 \pm 0.2$	$1.3 \pm 0.5$
4	$30 \pm 6$	$5.49 \pm 0.07$	$0.20 \pm 0.05$
5	$4 \pm 2$	$6.9 \pm 0.3$	$2 \pm 1$
6	$1.2 \pm 0.6$	$9.5 \pm 0.5$	$7 \pm 3$
7	$1.0 \pm 0.2$	$11.2 \pm 0.3$	$12 \pm 2$
8	$0.4 \pm 0.1$	$6.4 \pm 0.3$	$18 \pm 8$
9	$1.6 \pm 0.3$	$7.80 \pm 0.05$	$5 \pm 1$
10	$1.7 \pm 0.5$	$6.9 \pm 0.2$	$4 \pm 1$
11	$1.8 \pm 0.6$	$6.7 \pm 0.3$	$3 \pm 1$
12	$1.2 \pm 0.4$	$6.7 \pm 0.6$	$5 \pm 2$
13	$0.7 \pm 0.1$	$5.0 \pm 0.1$	$7 \pm 1$
14	$2 \pm 1$	$6.4 \pm 0.8$	$3 \pm 2$
15	$5 \pm 1$	$7.2 \pm 0.2$	$1.5 \pm 0.3$

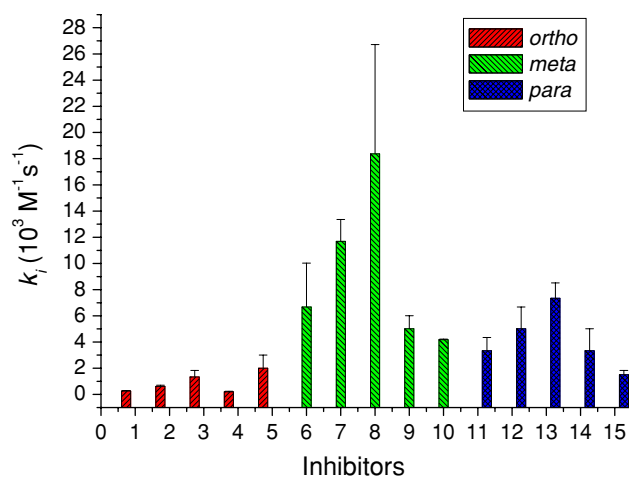
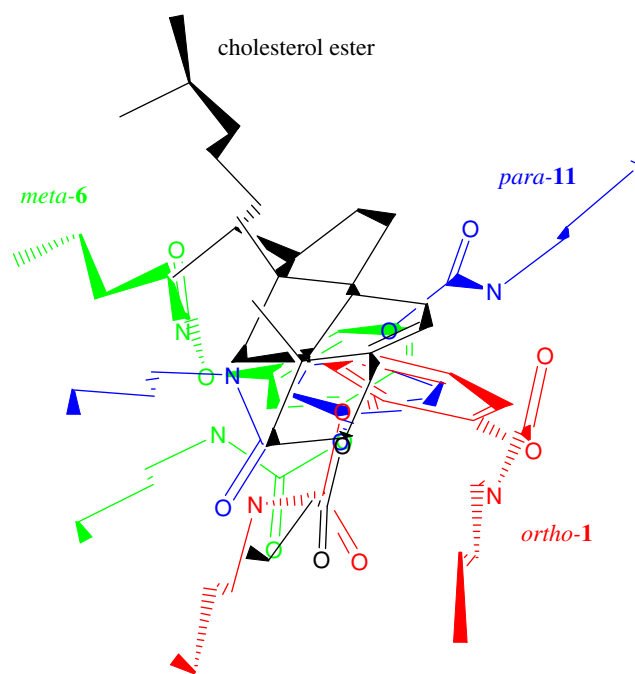
<sup>a</sup>  $K_i$  ( $1 + [S]/K_m$ ) values were obtained from the nonlinear least-squares curve fittings of  $k_{\text{app}}$  vs.  $[I]$  plot against Eq. 1 (Fig. 2) where  $[\text{PNPB}] = 100 \mu\text{M}$  and the  $K_m$  value for the CEase catalyzed hydrolysis of PNPB was  $100 \pm 20 \mu\text{M}$  which was calculated from Michaelis–Menten equation in the absence of any pseudo or alternate substrate inhibitor.  $k_i = k_2/K_i$

as the pseudo substrate inhibitors of CEase (Scheme 1), and the inhibition data are summarized in Table 1.

Since carbamates **1–15** are characterized as the pseudo substrate inhibitors of CEase, one carbamate group of carbamates **1–15** must bind to the acyl group binding site (ACS) of active site [4, 5], which is located deeply inside the enzyme. Meanwhile, the first step for this pseudo substrate inhibition is formation of the enzyme-inhibitor complex from an attack of the serine residue of the enzyme to one of the two carbamate carbonyl carbons of the inhibitor with the inhibition constant,  $K_i$ . The second step ( $k_2$ ) is the carbamylation step and formation of the carbamyl enzyme. That all  $k_2$  values are about the same (Table 1) indicates that the  $k_2$  step is basically independent upon the shape of the leaving group.

### 3.2 Comparisons of Inhibitory Potencies of CEase by Different Substituents on Carbamates **1–15**

When *n*-butyl, *n*-hexyl, *n*-octyl, *t*-butyl, and benzyl carbamate substituents are compared in a series of compounds such as benzene-1,2-di-*N*-substituted carbamates (**1–5**) (Fig. 1) for the CEase inhibition, the long chain substituted inhibitors are more potent than the short chain ones and more bulky inhibitors are less potent than less bulky ones (Table 1, Fig. 3). Since the shape of ACS of CEase looks

**Fig. 3** Comparisons of the  $k_i$  values of the CEase inhibitions by inhibitors **1–15****Fig. 4** Superimposition of cholesterol ester (black), *ortho*-1 (red), *meta*-6 (green), and *para*-11 (blue)

like a deep, narrow tunnel [4, 5], CEase binds preferably to the long chain inhibitors.

### 3.3 Comparisons of Inhibitory Potencies for CEase by *ortho* Carbamates **1–5**, *meta* Carbamates **6–10**, and *para* Carbamates **11–15**

In this paper, *ortho*, *meta*, and *para* benzene-di-substituted carbamates (**1–15**) are synthesized as the constrained analogs of *gauche*, *eclipsed*, and *anti* conformations for the glycerol backbones of triacylglycerol (substrate),



respectively (Fig. 1). Among *ortho*, *meta*, and *para* benzene-di-substituted carbamates such as compounds *ortho*-**3**, *meta*-**8**, and *para*-**13**, *meta* carbamates are always the most potent inhibitors of CEase (Table 1, Fig. 3). In other words, the best position for the second carbamate group of the above three inhibitors is 120° to the first carbamate group (Fig. 1). Accordingly, the glycerol backbone conformation in the enzyme-substrate tetrahedral complex prefers the *eclipsed* conformation. Meanwhile, superimposition of *ortho*, *meta*, and *para* inhibitors and the substrate cholesterol ester together indicates that *meta* inhibitor most resemble cholesterol ester (Fig. 4).

**Acknowledgement** We thank the National Science Council of Taiwan for financial support.

## References

- Lopez-Candales A, Bosner MS, Spilburg CA, Lange LG (1993) *Biochemistry* 32:12085–12089
- Wang C-S, Hartsuck JA (1993) *Biochim Biophys Acta* 1166:1–19
- Hui DY (1996) *Biochim Biophys Acta* 1302:1–14
- Wang X, Wang C-S, Tang J, Dyda F, Zhang XC (1997) *Structure* 5:1209–1218
- Chen JC-H, Miercke LJW, Krucinski J, Starr JR, Saenz G, Wang X, Spilburg CA, Lange LG, Ellsworth JL, Stroud RM (1998) *Biochemistry* 37:5107–5117
- Brodt-Eppley J, White P, Jenkins S, Hui D (1995) *Biochim Biophys Acta* 1272:69–72
- Auer J, Eber B (1999) *J Clin Basic Cardiol* 2:203–208
- Maron DJ, Fazio S, Linton MF (2000) *Circulation* 101:207–213
- Pioruńska-Stolzmann M, Pioruńska-Mikołajczak A (2002) *Pharm Res* 43:359–362
- Chiou S-Y, Lai G-W, Lin L-Y, Lin G (2006) *Ind J Biochem Biophys* 43:52–55
- Hosie L, Sutton LD, Quinn DM (1987) *J Biol Chem* 262:260–264
- Feaster SR, Lee K, Baker N, Hui DY, Quinn DM (1996) *Biochemistry* 35:16723–16734
- Feaster SR, Quinn DM (1997) *Meth Enzymol* 286:231–252
- Lin G, Shieh C-T, Ho H-C, Chouhwang J-Y, Lin W-Y, Lu C-P (1999) *Biochemistry* 38:9971–9981
- Lin G, Lin Y-F, Hwang M-T, Lin Y-Z (2004a) *Bioorg Med Chem Lett* 14:751–755
- Lin G, Yu G-Y (2005) *Bioorg Med Chem Lett* 15:2405–2408
- Lin M-C, Hwang M-T, Chang H-G, Lin C-S, Lin G (2007a) *J Biochem Mol Toxicol* 21:348–353
- Lin M-C, Hwang M-T, Chang H-G, Lin C-S, Lin G (2007b) *Eur J Lipid Sci Technol* 109:1104–1110
- Pietsch M, Gütschow M (2002) *J Biol Chem* 277:24006–24013
- Pietsch M, Gütschow M (2005) *J Med Chem* 48:8270–8288
- Lin G, Lin Y-F, Hwang M-T, Lin Y-Z (2004b) *Bioorg Med Chem Lett* 14:751–755